

Home Search Collections Journals About Contact us My IOPscience

High-responsivity UV detectors based on MgNiO films grown by magnetron sputtering

This content has been downloaded from IOPscience. Please scroll down to see the full text.

2014 EPL 106 38002

(http://iopscience.iop.org/0295-5075/106/3/38002)

View the table of contents for this issue, or go to the journal homepage for more

Download details:

IP Address: 129.187.254.47

This content was downloaded on 08/06/2014 at 17:49

Please note that terms and conditions apply.

EPL, **106** (2014) 38002

doi: 10.1209/0295-5075/106/38002

www.epljournal.org

## High-responsivity UV detectors based on MgNiO films grown by magnetron sputtering

Gaoming Li<sup>1</sup>, Jingwen Zhang<sup>1,2(a)</sup> and Xun Hou<sup>1,2</sup>

received 17 November 2013; accepted in final form 23 April 2014 published online 14 May 2014

PACS 85.60.Gz – Photodetectors (including infrared and CCD detectors)

PACS 81.05.Hd - Other semiconductors

Abstract – We have grown high-quality MgNiO films at 300 °C and 400 °C by the radio frequency magnetron sputtering. Transmittance measurements show that the absorption edges of the films grown at 300 °C and 400 °C are at 251 nm and 227 nm, respectively. We have deduced that the MgNiO film grown at a higher temperature has a higher Mg content and bigger bandgap. The XRD results confirm the deduction. Based on those films, we have fabricated UV detectors and measured the spectral response. The peak responsivities of the detectors with MgNiO films grown at 300 °C and 400 °C are located at 260 nm and 230 nm and are about 2.56 A/W and 2.3 A/W, respectively. The corresponding UV to visible rejection ratios (250 nm/500 nm) are 640 and 530, respectively. The large UV to visible rejection ratio and the high responsivity make the MgNiO-based detector a very encouraging candidate in the application of visible-blind and solar-blind UV light detection.

Copyright © EPLA, 2014

Introduction. – MgNiO is another competitive wide bandgap oxide semiconductor material [1–3], which has a great potential in photodetector [3–5] and transparent conductive film [6], just like MgZnO. Its bandgap can be tuned from 3.5 eV (NiO) to 7.8 eV (MgO) [3] and is nearly linear with the composition of MgNiO [2]. Moreover, the ternary solution  $Mg_xNi_{1-x}O$  is always rock salt structured, as x varies from 0 to 1 continuously [7]. Because the ionic radii of Ni<sup>2+</sup> and Mg<sup>2+</sup> are very close, they substitute each other readily in the solution. And the lattice constant of  $Mg_xNi_{1-x}O$  follows Vegard's rule, it is also a linear function of the composition. The rock salt structure belongs to the cubic crystal group, so it does not exhibit piezoelectric effect and polarization field for its inversion symmetry [3]. This is important in bandgap engineering. All of these merits discussed above make MgNiO a promising choice in ultraviolet application.

MgNiO can just be seen as NiO incorporated with Mg. Actually, NiO is an inborn p-type material [8]. This amazing point just slakes the thirst for seeking p-type material in wide bandgap oxide semiconductors. Ni $^{3+}$  ion

 ${}^{\rm (a)}{\rm E\text{-}mail:}~{\tt jwzhang@mail.xjtu.edu.cn}$ 

plays a significant role in the contribution to the conductivity of NiO. The appearance of a Ni<sup>3+</sup> ion is always a concomitant of the formation of Ni vacancy [9]. The addition of a monovalent atom such as Li can increase the conductance of NiO. With the p-type MgNiO, many optoelectronic devices based on a p-n structure or on a p-i-n structure can be achieved. Recently, some researches about the p-n heterojunction diode based on NiO have been reported [10,11]. There are also reports on MgNiObased UV detectors [3–5]. However, in their study they did not give out the responsivity which is an important parameter for photodetectors and can be used to characterize the photoelectric conversion efficiency of optoelectronic devices. In addition, detectors based on other oxide semiconductors such as zinc oxide can also realize a highly sensitive detection of UV light or gas, and very large sensitivities to ozone and methane have been achieved [12,13]. However, it is not possible to fabricate solar-blind detectors based on undoped ZnO. That is why we need MgZnO or MgNiO for solar-blind detection.

In this paper, we fabricated high-performance Metal-Semiconductor-Metal (MSM) UV detectors based on a MgNiO film grown by Radio Frequency (RF) magnetron

<sup>&</sup>lt;sup>1</sup> Department of Electronic Science and Technology, Xi'an Jiaotong University - No. 28 Xianning West Road, 710049 Xi'an, China

<sup>&</sup>lt;sup>2</sup> Key Laboratory for Physical Electronics and Devices of the Ministry of Education, Xi'an Jiaotong University No. 28 Xianning West Road, 710049 Xi'an, China

sputtering, a cost-effective method which is more suitable for mass production. In the previous works mentioned above, the MgNiO film was grown by Molecular Beam Epitaxy (MBE) [4] or Electron Beam Evaporation (EBE) [5]. We found that a MgNiO film grown at higher temperature had a richer Mg content. And the responsivity spectra of the detectors were also acquired.

**Experiments.** – The sputtering target was a  ${\rm Mg_{0.2}Ni_{0.8}O}$  ceramic wafer with purity of 99.99%. Its diameter was 75 mm and it was 5 mm thick. The target was placed parallel to the sample holder with a distance of 70 mm. We used 2 inch quartz glass substrates and they were rinsed, respectively, in acetone, ethanol and deionized water before sputtering, 10 minutes for each step. The base pressure was  $3.6\times10^{-4}\,{\rm Pa.}$  O<sub>2</sub> and Ar with a flow rate of 35 sccm and 25 sccm, respectively, were the sputtering gas. The sputtering pressure was  $1.2\,{\rm Pa.}$  The RF power with the frequency at  $13.56\,{\rm MHz}$  was  $100\,{\rm W.}$  The substrate was heated at  $300\,{\rm ^{\circ}C}$  and  $400\,{\rm ^{\circ}C}$ , respectively, during sputtering. Pre-sputtering lasted  $10\,{\rm min}$ , sputtering process lasted  $1\,{\rm h.}$ 

After the film growth, the MSM photodetector was fabricated by the standard lift-off technique. An Al interdigitated electrode was evaporated on the MgNiO film and the thickness of the electrode was about 100 nm. There were 50 pairs of interdigital (IDT) electrodes in the photoconductive detector. Each electrode finger was 500  $\mu \rm m$  long and 15  $\mu \rm m$  wide, the spacing between the two neighboring fingers was 30  $\mu \rm m$ . There was a total photosensitive area of  $1.24\times 10^{-2}\,\rm cm^2$  of the detector. The interdigitated electrodes have a high efficiency to collect photon-generated carriers.

The transmittance spectrum of the MgNiO film was measured by a Varian UV-vis spectrophotometer (Cary 5000). An X-ray  $2\theta$ - $\theta$  scan using a Cu K<sub>\alpha</sub>1 source ( $\lambda$  = 0.154056 nm) was employed to characterize the orientation of the MgNiO film, and the Rigaku D/MAX-2400 diffractometer was used. The scanning electron microscope (JSM 6700F) and atom force microscope (Digital Instruments D5000) were employed to characterize the surface morphology. The current and voltage (I-V) curves of MSM UV photodetectors under UV illumination and without UV illumination were measured by a Keithley picoammeter (modal 6487). The MÜLLER ELEKTRONIK OP-TIK xenon lamp (TYP LAX 1450) was used as light source. And an ACTON RESEARCH CO. monochromator (SP2150i) and a Stanford Research Systems optical chopper (Model SR 540) were needed. The responsivity spectrum of the UV photodetectors was measured by a Stanford Research Systems DSP lock-in amplifier (Model SR 830).

Results and discussion. – The transmittance spectra of MgNiO films grown at  $300\,^{\circ}\text{C}$  and  $400\,^{\circ}\text{C}$  are shown in fig. 1. We can see from the results that MgNiO films have a high transmittance in the wavelength range from about  $400\,\text{nm}$  to  $800\,\text{nm}$  which corresponds to a visible

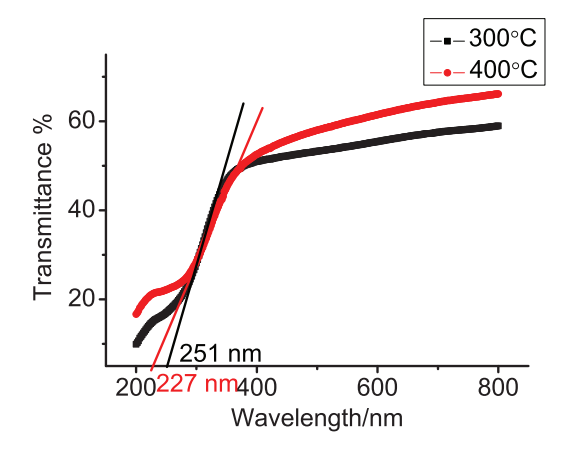


Fig. 1: (Colour on-line) Transmittance of MgNiO films grown at 300  $^{\circ}\mathrm{C}$  and 400  $^{\circ}\mathrm{C}$  .

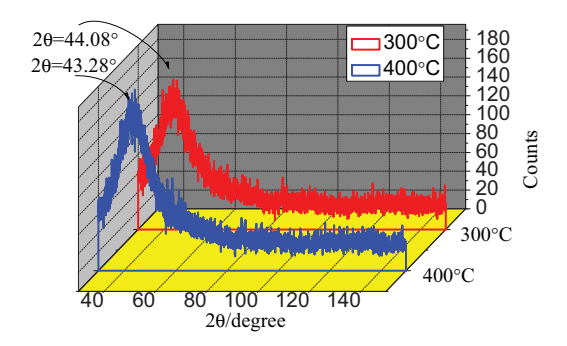


Fig. 2: (Colour on-line) XRD results of MgNiO films grown at  $300\,^{\circ}\mathrm{C}$  and  $400\,^{\circ}\mathrm{C}.$ 

light wavelength due to the wide bandgap. Strong intrinsic absorption occurs at 300 nm below. The absorption edges are also shown in fig. 1. Through (1), we can approximately estimate the bandgap of the film:

$$E_g = 1240/\lambda. (1)$$

 $E_g$  refers to the bandgap in eV, and  $\lambda$  denotes the wavelength in nm. The MgNiO film with growth temperature of 400 °C has an absorption edge at 227 nm, the corresponding bandgap is 5.46 eV. Otherwise, the film grown at 300 °C has an absorption edge at 251 nm, the bandgap is only 4.94 eV. From Vegard's law, the bandgap and other parameters such as the lattice constant of the solid solution are linear with the constituent content described by

$$E_g(A_m B_n) = m E_g(A) + n E_g(B). \tag{2}$$

Thus, the content of Mg in the film grown at  $400\,^{\circ}\mathrm{C}$  is 0.46, namely the solution can be expressed as  $\mathrm{Mg_{0.46}Ni_{0.54}O}$ . The content of Mg in the film grown at  $300\,^{\circ}\mathrm{C}$  is 0.33,  $\mathrm{Mg_{0.33}Ni_{0.67}O}$  can denote that solution. It is interesting to find that the Mg content in both films are bigger than that in the sputtering target, the Mg content of which is only 0.2. It is evident that there is a Mg enrichment phenomenon when heating the substrate during the sputtering process. And the higher the growth temperature is, the bigger the content of Mg is. A similar

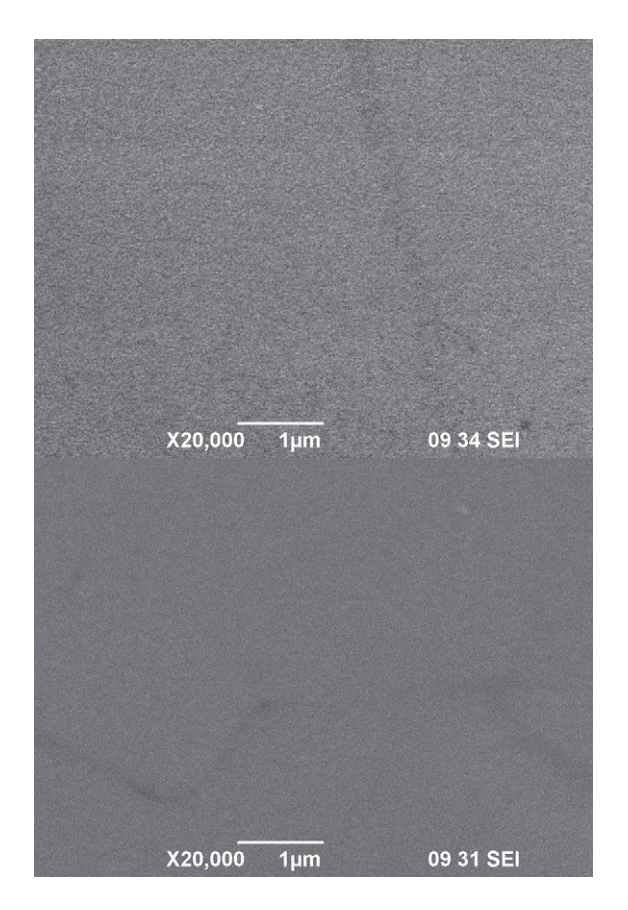


Fig. 3: SEM images of MgNiO films grown at 300  $^{\circ}$ C (top) and 400  $^{\circ}$ C (bottom).

phenomenon has been found in the growth of a MgZnO film by sputtering [14].

The XRD results are shown in fig. 2. The diffraction peaks  $(2\theta)$  are located at  $44.08^{\circ}$  and  $43.28^{\circ}$  for MgNiO films grown at  $300\,^{\circ}\mathrm{C}$  and  $400\,^{\circ}\mathrm{C}$ , respectively. These peaks correspond to (200) lattice planes, the interplanar spacing between which is  $2.097\,\text{Å}$ . The bigger  $2\theta$  of the peak for the film grown at  $300\,^{\circ}\mathrm{C}$  than that for the film grown at  $400\,^{\circ}\mathrm{C}$  corroborates our deduction that the MgNiO film grown at a higher temperature has a higher content of Mg. As the interplanar spacing of MgO (200) lattice planes is  $2.106\,\text{Å}$ , and the one of NiO (200) lattice planes is  $2.088\,\text{Å}$  [15], then based on Vegard's law on lattice constant, the MgNiO film with higher Mg content has a bigger interplanar spacing, thus a smaller  $2\theta$  diffraction peak.

The SEM images of the MgNiO films are shown in fig. 3. The growth temperature does not influence the surface morphology much according to the images. Grain boundary can be seen in the images too, that is to say the MgNiO film grown by RF magnetron sputtering is polycrystalline. The EDS data of the films are shown in fig. 4. The Si  $K_{\alpha}$  peak and part of the O  $K_{\alpha}$  peak originate from the quartz glass substrate. The atom percentages also indicate that the film grown at 400 °C has larger Mg content than the one grown at 300 °C, although the data of Mg content are

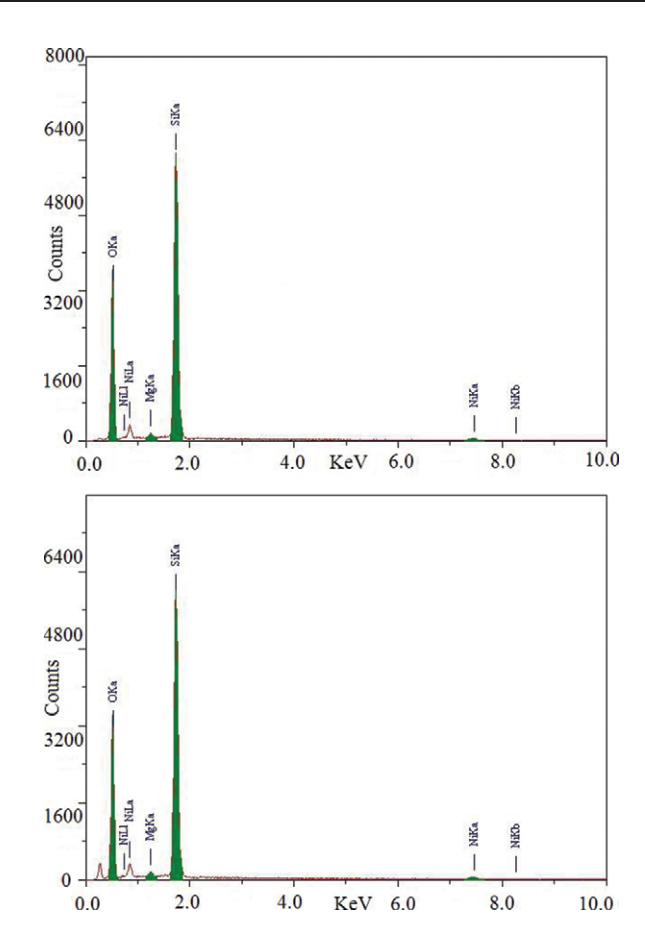


Fig. 4: (Colour on-line) EDS data of MgNiO films grown at 300 °C (top) and 400 °C (bottom).

a little different from those deriving from transmittance results and Vegard's law.

As we know, surface roughness and crystallite size of the active layer of the detector have important impact on the detector's performance. The dependences of detector's sensitivity on the film structure and surface roughness have been discussed in detail by some researchers [12,13]. The AFM images of the films are shown in fig. 5. The roughnesses of the films grown at 300 °C and 400 °C are 7.56 nm and 0.78 nm, respectively. The corresponding crystallite sizes are about 350 nm and 50 nm, respectively.

The I-V curves of MgNiO detectors are shown in fig. 6. The wavelength of the light source is 254 nm and the light intensity is  $1.56\,\mu\text{W}/\text{cm}^2$ . For the detector based on the MgNiO film grown at 400 °C, the dark current and photocurrent at 5 V are 47.1 nA and 65.7 nA, respectively. And the detector with the MgNiO film grown at 300 °C has a higher dark current and a higher photocurrent which are 135 nA and 173 nA, respectively. Apparently, there is a low photocurrent to dark current ratio because the intensity at that wavelength of the light source is weak.

The spectral response of the detector with  $400\,^{\circ}\mathrm{C}$  MgNiO film is shown in fig. 7 (top). The peak responsivity is at  $230\,\mathrm{nm}$  and is about  $2.56\,\mathrm{A/W}$ . From fig. 7 (bottom) we see that the peak responsivity of the detector

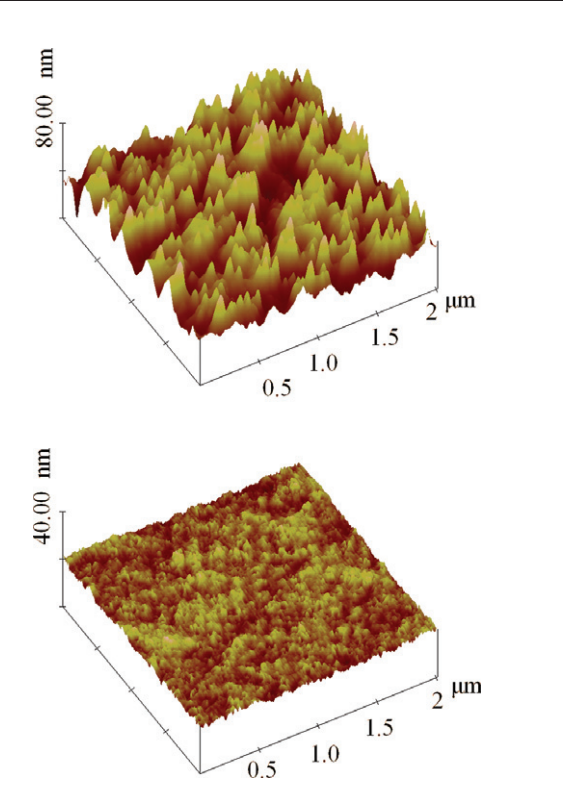


Fig. 5: (Colour on-line) AFM images of MgNiO films grown at  $300\,^{\circ}\mathrm{C}$  (top) and  $400\,^{\circ}\mathrm{C}$  (bottom).

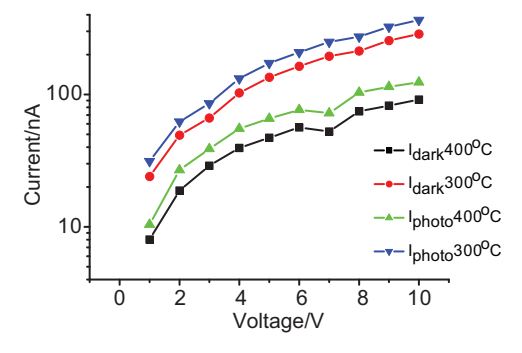


Fig. 6: (Colour on-line) I-V curves of detectors based on MgNiO films.

with 300 °C MgNiO film is located at 260 nm and is about 2.3 A/W. These experiment results are in accordance with the results of transmittance and XRD. This corroborates the conclusion that the MgNiO film grown at a high temperature has a higher Mg content, so its bandgap is bigger. Thus the detector based on that film has a shorter peak responsivity wavelength. That is why the peak responsivity wavelength of the detector based on the 400 °C MgNiO film located at 230 nm is shorter than that of the detector with the 300 °C MgNiO film located at 260 nm. Moreover, we notice that the peak wavelength is close to the absorption edge. For the 400 °C MgNiO film the absorption edge is 227 nm and the peak responsivity wavelength is 230 nm; for the 300 °C MgNiO film the absorption edge is 251 nm

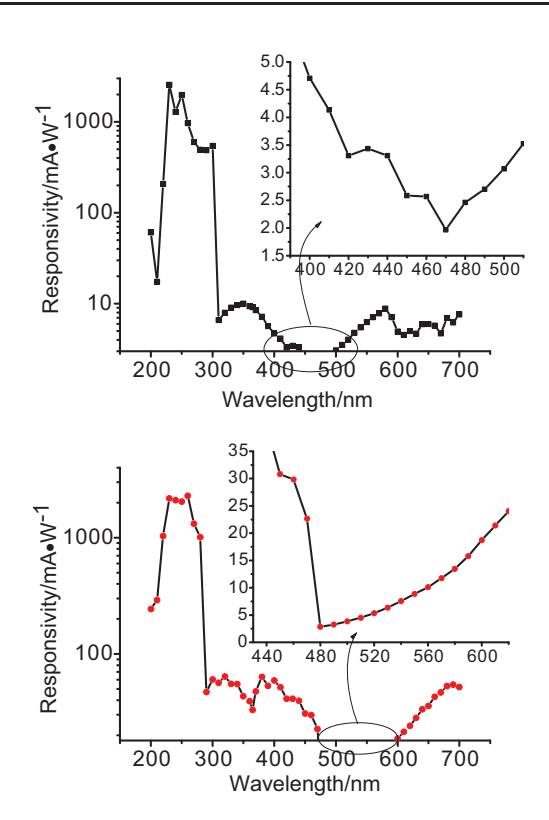


Fig. 7: (Colour on-line) Spectral response of detectors with 400 °C MgNiO films (top) and 300 °C MgNiO films (bottom).

and the peak responsivity wavelength is 260 nm. That is to say, the intrinsic transition from the top of the valence band to the bottom of the conductance band is the main mechanism in the processes of light absorption and photoresponse. This can also explain why the photocurrent of the detector based on the 300 °C MgNiO film is larger than that of the detector based on the 400 °C MgNiO film. Because the wavelength used in the I-V curve measurement is 254 nm, which is closer to the peak responsivity wavelength of the detector with the 300 °C MgNiO film than to that of the detector with the 400 °C MgNiO film. Thus, at 254 nm the detector with the 300 °C MgNiO film has a bigger responsivity. At last, we can acquire a high UV to visible rejection ratio which is nearly two orders of magnitude for both detectors. This is very promising in the application of visible-blind and solar-blind UV light detection. Actually, the rejection ratio can be used to depict the sensitivity of the detector. The sensitivity is highly dependent on the surface morphology, film structure and resistivity. A ZnO-based gas sensor even can attain a high on/off ratio of 8 orders of magnitude [13].

Conclusion. – In summary, high-quality MgNiO films grown at 300 °C and 400 °C are achieved by the radio frequency magnetron sputtering. Then we have employed transmittance measurement, XRD and SEM to characterize the films. The results show that the MgNiO film grown at a higher temperature has a larger Mg content, so a bigger bandgap. The detectors based on those films

are fabricated by the standard lift-off technique. We have measured the I-V curves and spectral response of the detectors. The peak responsivities of detectors based on MgNiO films grown at 300 °C and 400 °C are located at 260 nm and 230 nm, and they are about 2.56 A/W and 2.3 A/W, respectively. The detectors are very promising in the application of visible-blind and solar-blind UV light detection.

\* \* \*

This work was supported in part by the Project of the National Natural Science Foundation of China under Grant No. 61176018-F040104.

## REFERENCES

- ZAANEN J., SAWATZKY G. A. and ALLEN J. W., Phys. Rev. Lett., 55 (1985) 418.
- [2] JI Z., HE Z., LIU K., ZHAO S. and HE Z., J. Cryst. Growth, 273 (2005) 446.
- [3] MARES J. W., BOUTWELL C. R., SCHEURER A., FALANGA M. and SCHOENFELD W. V., Proc. SPIE, 7603 (2010) 76031B.
- [4] MARES J. W., BOUTWELL R. C., WEI M., SCHEURER A. and SCHOENFELD M. V., Appl. Phys. Lett., 97 (2010) 161113.

- [5] ZHAO Y., ZHANG J., JIANG D., SHAN C., ZHANG Z., YAO B., ZHANG D. and SHEN D., J. Phys. D: Appl. Phys., 42 (2009) 092007.
- [6] SALEM A. M., MOKHTAR M. and EL-SHOBAKY G. A., Solid State Ion., 170 (2004) 33.
- [7] KUZMIN A. and MIRONOVA N., J. Phys.: Condens. Matter, 10 (1998) 7937.
- [8] JOSHI U. S., MATSUMOTO Y., ITAKA K., SUMIYA M. and KOINUMA H., Appl. Surf. Sci., 252 (2006) 2524.
- [9] ADLER D. and FEINLEIB J., Phys. Rev. B, 2 (1970) 3112.
- [10] WONG H. F., WONG K. H. and LAU C. H., Phys. Status Solidi A: Appl. Mater., 206 (2009) 2202.
- [11] OHTA H., HIRANO M., NAKAHARA K., MARUTA H., TANABE T., KAMIYA M., KAMIYA T. and HOSONO H., Appl. Phys. Lett., 83 (2003) 1029.
- [12] NUNES P., FORTUNATO E., LOPES A. and MARTINS R., Int. J. Inorg. Mater., 3 (2001) 1129.
- [13] Bender M., Fortunato E., Nunes P., Ferreira I., Marques A., Martins R., Katsarakis N., Cimalla V. and Kiriakidis G., *Jpn. J. Appl. Phys.*, **42** (2003) L435.
- [14] JAGADISH C. and PEARTON S., Zinc Oxide Bulk, Thin Films and Nanostructures: Processing, Properties, and Applications (Elsevier, Amsterdam) 2006, p. 114.
- [15] MORRIS M. C., Powder Diffraction Data: From the Joint Committee on Powder Diffraction Standards Associateship at the National Bureau of Standards: Data Book (Joint Committee on Powder Diffraction Standards, Swarthmore) 1976.